



# Assessing salinity hazards in coastal aquifers: implications of temperature boundary conditions on aquifer–ocean interaction

Ismail Abd-Elaty<sup>1</sup> · Alban Kuriqi<sup>2,3</sup> · Ashraf Ahmed<sup>4</sup>

Received: 8 June 2023 / Accepted: 3 March 2024  
© The Author(s) 2024

## Abstract

Investigating the repercussions of climate change and irrigation timing on groundwater contamination necessitates thorough examination of the fluctuations in seawater and groundwater recharge temperature. This study introduces an innovative numerical approach to analyze groundwater salinity and temperature dynamics across three distinct scenarios using the SEAWAT code based on Henry's problem. The first scenario delves into the impact of seawater temperature, the second focuses on the consequences of aquifer freshwater recharge temperature, and the third amalgamates the effects of both scenarios. Remarkably, the study reveals that saltwater intrusion (SWI) experiences a decline attributable to the aquifer's heightened seawater temperature and the diminished inland freshwater temperature. Furthermore, combining these two scenarios has a more pronounced effect on aquifer pollution; the temperature-induced changes in SWI for this third scenario reach + 8.10%, + 12.70%, + 16.20%, + 24.90%, + 28.30%, and + 31.80% compared to the case without considering the temperature effect. Notably, our results propose a potential strategy to mitigate SWI by introducing cold freshwater recharge into aquifers, such as irrigation at night time when water temperature is low. This innovative approach underscores the interconnectedness of various environmental factors. It provides a practical avenue for proactive intervention in safeguarding groundwater quality against the adverse impacts of climate change and irrigation practices.

**Keywords** Climate change · SEAWAT · Aquifer and ocean temperature · Seawater intrusion control

## Abbreviations

2D Two dimensions  
3D Three dimensions

ADCI Abstraction of brackish water, Desalination, Cooling the desalinated water, and Injection into the aquifer  
ET Evapotranspiration  
FEFLOW Finite element to simulate flow, mass, and heat transport processes in the sub-surface flow system  
FSGD Fresh submarine groundwater discharge  
HST3D A computer code for simulation of heat and solute transport in three-dimensional groundwater flow systems  
GWT Groundwater temperature  
LST Land surface temperature  
HYDROCOIN Hydrologic code intercomparison  
IPCC Intergovernmental panel on climate change  
IMT Integrated MT3DMS Transport  
MODFLOW United States geological survey modular finite-difference flow model  
MT3DMS Modular transport three-dimensional multi-species  
MSL Mean sea level

✉ Ismail Abd-Elaty  
Eng\_abdelaty2006@yahoo.com

✉ Ashraf Ahmed  
Ashraf.ahmed@brunel.ac.uk

Alban Kuriqi  
alban.kuriqi@tecnico.ulisboa.pt

<sup>1</sup> Department of Water and Water Structures Engineering, Faculty of Engineering, Zagazig University, Zagazig 44519, Egypt

<sup>2</sup> CERIS, Instituto Superior Técnico, Universidade de Lisboa, Av. Rovisco Pais 1, 1049-001 Lisbon, Portugal

<sup>3</sup> Civil Engineering Department, University for Business and Technology, 10000 Pristina, Kosovo

<sup>4</sup> Department of Civil and Environmental Engineering, Brunel University London, Kingston Lane, Uxbridge, Sussex UB83PH, UK

MOCDENSE	A two-constituent solute transport model for groundwater
SEAWAT	Three-dimensional variable-density groundwater flow
SLR	Sea-level rise
SWI	Saltwater intrusion
SUTRA	Saturated–unsaturated variable-density groundwater flow with solute or energy transport
SUTRA-MS	SUTRA-simulate heat and multiple-solute transport
SWIFT	Three-dimensional Model to Simulate Groundwater Flow, Heat, Brine, and Radionuclide Transport
TOUGH2	Multi-dimensional numerical models for simulating the coupled transport of water, vapor, non-condensable gas, and heat in porous and fractured media
USA	United States of America
VDF	Variable-density flow

## Introduction

Aquifer–ocean temperature contrasts are common worldwide. They affect flow and salinity distributions in unconfined coastal aquifers (Nguyen et al. 2020). Water scarcity problems are caused by several factors, including ecosystem degradation, over-pumping, overpopulation, climate change, and pollution (Rosegrant et al. 2002; Abd-Elaty et al. 2024). In arid and semi-arid regions with limited annual rainfall, groundwater is the primary water source for agriculture, industry, and domestic use (Todd and Mays 2004). The most densely populated regions in the world are coastal zones, with 53% of the world's population living within 200 km of the coast; these areas are subjected to serious hydrological problems such as the shortage of freshwater, groundwater contamination, and seawater intrusion (SWI) (Abd-Elaty et al. 2021b; Bear 2012).

Coastal fresh groundwater management is a challenging research topic due to the relevance of these resources and the enormous risks due to global change and overpopulation (Abd-Elaty et al. 2021b; Bear 2012).

Groundwater is a relatively stable source since climate fluctuations usually induce relatively small variations in groundwater levels. A large volume of water stored in aquifers may serve as a buffer to supply water during prolonged drought periods (Bear and Cheng 2010). SWI occurs when saline water displaces freshwater in aquifers. This

phenomenon occurs not only in coastal aquifers from seawater invasion but also in shallow aquifers from the discharge of surface waste and deep aquifers from the advance of salt water of geologic origin (Abd-Elaty et al. 2021a; Todd and Mays 2004).

The Intergovernmental Panel on Climate Change (IPCC, 2007) showed that the sea-level rise (SLR) was predicted to be 18–58 cm, with a rate of rising 8–16 mm year<sup>-1</sup> from 2081 to 2100 (IPCC, 2014). Around 95% of the world's coastal areas will be severely affected by SLR by 2100, increasing the risk of flooding and SWI (Agren and Svensson, 2007).

SLR is among the most important consequences of global climate change and is widely acknowledged as a major threat to many countries. About 10% of our planet's total population lives in coastal regions and will likely face increasingly frequent inundation events and eventually become permanently flooded (Carrasco et al., 2016). Abd-Elaty et al. (2022) studied the impact of climate change on SLR and the reduction in fresh groundwater recharge on SWI in a coastal aquifer. The results showed that aquifer salinity significantly influences boundary conditions. Mazhar et al. (2022) studied the effect of salinization caused by SLR on the biological processes of coastal soils. The results showed that the biological activity of soils affected by SLR is certainly needed in both the short and long terms. Zhu et al. (2023) developed an experimental analysis of the pumping effect on SWI, the results of intermittent and constant pumping for the same total extraction rate, showing that intermittent pumping caused earlier well salinization compared to constant pumping. However, the aquifer contained a greater mass of salt under constant pumping.

Since 1964, the variations of Henry's problem (1964) have been solved (Simpson and Clement 2004), including a temperature–salinity developed numerically and laboratory by Henry and Hilleke (1972). Xin et al. (2023) presented the impact of cooling fresh groundwater recharge on SWI in coastal aquifers. The decreasing groundwater temperature (by extracting fresh groundwater from and recharging cooled and more viscous water back into coastal aquifers) can relieve seawater intrusion and lead to safe exploitation of the fresh submarine groundwater discharge (FSGD) based on laboratory experiments and numerical simulations. Benz et al. (2017) estimated the land surface temperature (LST) and shallow groundwater temperature (GWTs) (Fig. 1), the study showed that the regions where snow cover is decreasing, the offset between GWTs and LST will decrease, and the GWTs will increase at a slower rate than LST. Also, the study showed that GWTs are warmer than

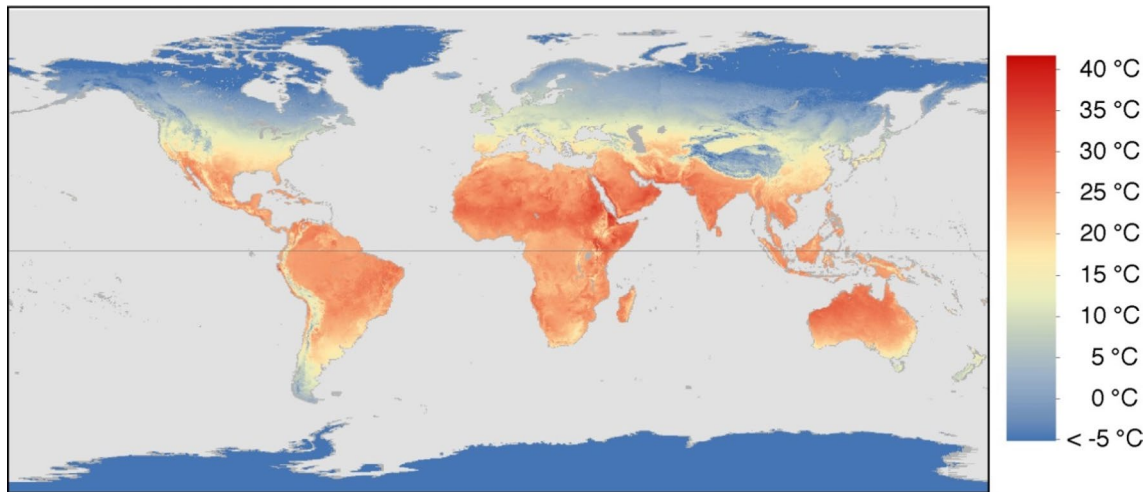


**Fig. 1** Global map of shallow groundwater temperature (Benz et al. 2017)

LST in 83% of all measurement points. The average offset is  $1.2 \pm 1.5$  K with highest offset in both the warmest and coldest areas of Earth. Also, the regions where the offset is predominantly dictated by evapotranspiration (ET), declining ET will decrease the offset and reduce GWTs increase otherwise in rising ET.

Dausman et al. (2010) compared the numerical model results of SEAWAT V.4 with the laboratory experiment of Henry and Hilleke (1972) for solute and heat transport. The experiment used a large sand tank to recharge warm freshwater. At the same time, the cold saline water boundary was represented on the one side. The experiment observed a narrow transition zone between the saltwater and freshwater flow systems. It displayed a good agreement with the SEAWAT simulation. Langevin (2007) showed that aquifers' temperature distribution might change due to groundwater flow patterns due to the effects of density and viscosity, where the freshwater density changes from 1000 to  $999.6 \text{ kg/m}^3$  by increasing the temperature by  $10\text{ }^\circ\text{C}$ . Decreasing the density can significantly affect groundwater flow (Henry and Hilleke 1972). Van Lopik et al. (2015) studied salinization induced by heat transfer from well casings in a stratified aquifer. The study concluded that the heat loss from hot well casings should be considered when monitoring long-term changes in groundwater quality near wells where hot liquids or gases are transported.

Pu et al. (2021) investigated the effect of artificial freshwater recharge temperature on SWI, and the restoration salinized using experimental and numerical studies. The results showed that cold freshwater recharge performs better compared with water in mitigating SWI. Hot freshwater

recharge induces a marked overshoot of salinity distribution: Seawater retreats first but intrudes until a steady state. Yu et al. (2022) studied the impact of thermal in heterogeneous coastal aquifers on flow and salinity distributions; the study showed that the warmer freshwater could lead to a significant landward intrusion of the freshwater–seawater interface in the heterogeneous aquifer. Nandimandalam et al. (2023) studied the impact of sea surface temperature anomaly for 2017, 2018, and 2019, which varies between  $21\text{--}39\text{ }^\circ\text{C}$ ,  $15\text{--}34\text{ }^\circ\text{C}$ , and  $20\text{--}39\text{ }^\circ\text{C}$  which impact on SWI in the coastal Andhra Pradesh region in India using field investigation by a total of 234 water samples. Abd-Elaty et al. (2023) mitigated SWI in coastal aquifers using injection of freshwater cooling. The study developed a new method using Abstraction of brackish water, Desalination, Cooling the desalinated water, and Injection into the aquifer (ADCI) strategy; the results recommended that the irrigation can be done at night when freshwater temperatures are low.

Climate change impacts the surface water temperature in oceans and the freshwater used in the irrigation process. The simulation of groundwater systems may require studying how changing the groundwater temperature affects variable-density flow in coastal aquifers. Therefore, this study aims to present a new simulation for a hypothetical case of Henry's problem, considering the effect of temperature on SWI. The current study is developed to investigate the changing of seawater and aquifer freshwater recharge boundary temperature by  $10\text{ }^\circ\text{C}$ ,  $15\text{ }^\circ\text{C}$ ,  $20\text{ }^\circ\text{C}$ ,  $30\text{ }^\circ\text{C}$ ,  $35\text{ }^\circ\text{C}$ , and  $40\text{ }^\circ\text{C}$  influencing groundwater contamination by SWI in coastal aquifers.

**Table 1** The parameters used for the Henry–Hilleke problem and Henry's problem (Dausman et al. 2010) and Henry's problem (Guo and Langevin 2002)

Parameter	Henry–Hilleke problem	Henry's problem	Units
	Values		
Saltwater head ( $h_s$ )	1	1	m
Inland freshwater flux ( $q_{in}$ )	7.20	5.702	$\text{m}^3 \text{ day}^{-1} \text{ m}^{-1}$
Saltwater density ( $\rho_s$ )	1025	1025	$\text{kg m}^{-3}$
Freshwater density ( $\rho_f$ )	1000	1000	$\text{kg m}^{-3}$
Specific storage	0	0	$\text{m}^{-1}$
Longitudinal dispersivity ( $\alpha_L$ )	0	0	m
Transverse dispersivity ( $\alpha_T$ )	0	0	m
Molecular diffusion coefficient ( $D^*$ )	2.0571	0.57024	$\text{m}^2 \text{ day}^{-1}$
Thermal diffusivity ( $D^*$ )	20.571	20.571	$\text{m}^2 \text{ day}^{-1}$
Saltwater concentration ( $C$ )	35,700	35,700	$\text{mg L}^{-1}$
Hydraulic conductivity ( $k$ ) (Isotropic)	864	864	$\text{m}^{-1} \text{ day}$
Porosity ( $n$ )	0.35	0.35	Dimensionless
Reference kinematic viscosity	0.0864	0.0864	$\text{m}^2 \text{ day}^{-1}$
Reference dynamic viscosity	86.4	86.4	$\text{Kg m}^{-1} \text{ d}^{-1}$
Reference concentration	0	0	$\text{mg L}^{-1}$
Reference temperature	25°	25°	c
Density changes with concentration	0.715	0.715	Dimensionless
Density changes with temperature	-0.375	-0.375	Dimensionless

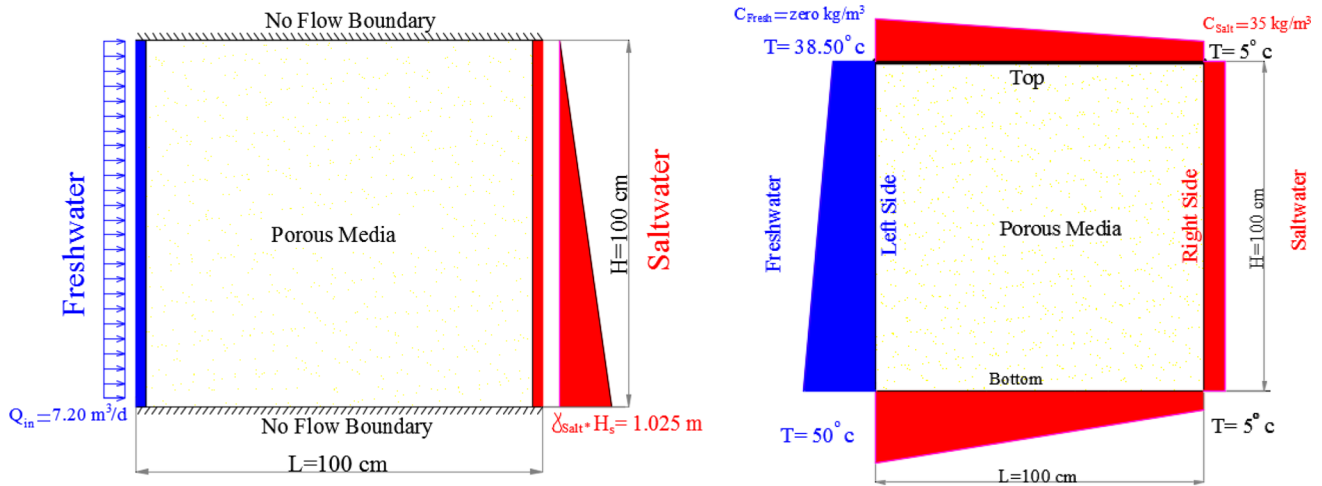


**Fig. 2** Henry and Hilleke problem boundary condition for head (left) and concentration (right)

## Materials and methods

### Coupled fluid flow and solute transport model

The 3D variable density of groundwater flow coupled with multi-species of solute and heat transport of SEAWAT V.4 was used in the current study. This updated version of SEAWAT (Guo and Langevin, 2002; Langevin and others, 2003), was designed to calculate fluid density and viscosity as a function of one or more species, and heat

can be represented as one of the species. The variable-density flow (VDF) process solves the variable-density flow equation in the freshwater head (Guo and Langevin 2002). The Integrated MT3DMS Transport (IMT) process solves the advection–dispersion equation (Zheng and Wang 1999). The governing equation of the heat transport equation which was manipulated by (Thorne et al. 2006) to highlight the similarity with the solute transport equation. This code follows a modular structure; thus, new capabilities can be added with only minor modifications to the main program. SEAWAT reads and writes standard MODFLOW

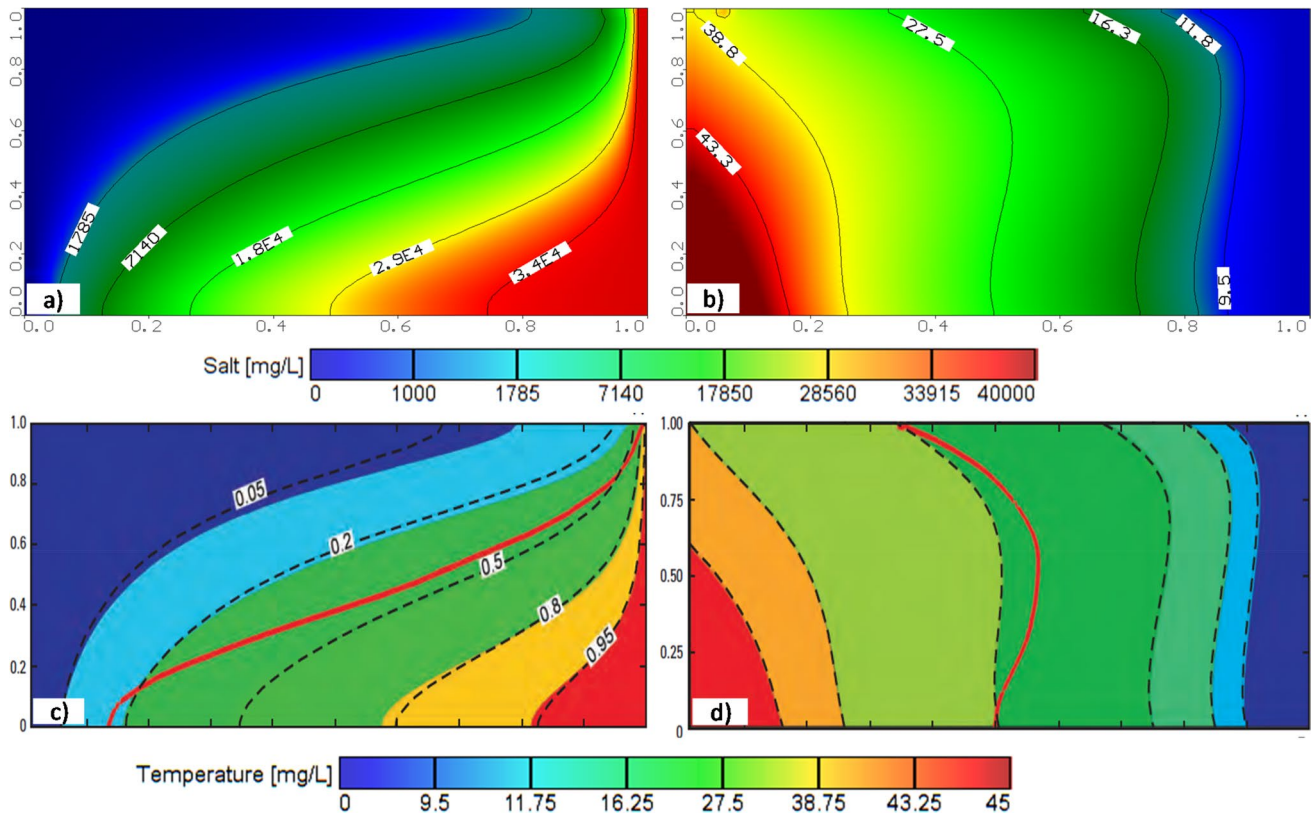


**Fig. 3** Isochlor of modeling results for: **a** SEAWAT\_V4 for concentration, **b** SEAWAT\_V4 for temperature, and **c** and **d** concentration and temperatures, respectively, for SUTRA-MS results in color shading by the solid black lines, numerical solution by Henry and Hilleke

(1972) shown as the 50% concentration contour and the 27.5 °C temperature contour by the solid red line, and the solution by HST3D results shown as the dashed black line (Hughes and Sanford 2004)

and MT3DMS data sets, although some extra input may be required for some SEAWAT simulations. This means that many existing pre- and post-processors can be used to create input data sets and analyze simulation results. Users familiar with MODFLOW and MT3DMS should have little difficulty applying SEAWAT to problems of variable-density groundwater flow (Guo and Langevin 2002).

SEAWAT (Guo and Langevin 2002) also accurately simulates the Henry problem, and SEAWAT results compare well with those of SUTRA (Voss 1984). The Elder problem is a complex flow system in which fluid flow is driven solely by density variations. Results from SEAWAT, for six different times, compare well with results from Elder's original solution and results from SUTRA. The HYDROCOIN problem consists of fresh groundwater flowing over a salt dome. Simulated salinity contours compare well for SEAWAT and MOCDENSE (Sanford and Konikow 1985).

One of the powerful new options in SEAWAT-2000 is the capability to use the VDF process without simulating solute transport. This option could be used for many coastal groundwater flow models that require accurate ocean boundary representation but do not require simulation of saltwater intrusion. This approach can substantially shorten computer runtimes because time step lengths are not restricted by stability criteria necessary for accurate transport solutions. This improvement allows users to quickly change simulation options without changing the input files (Guo and Langevin 2002).

Also, it can simulate solute and heat transport simultaneously, as well as the effect that fluid viscosity variations have on resistance to groundwater flow (Langevin et al. 2008).

The variable-density flow (VDF) process solves the variable-density flow equation in terms of the freshwater head (Guo and Langevin 2002), Eq. 1:

$$\begin{aligned} \nabla \left[ \rho \frac{\mu_o}{\mu} K_o \left( \nabla h_o + \frac{\rho - \rho_o}{\rho_o} \nabla z \right) \right] \\ = \rho S_{s,0} \left( \frac{\partial h_o}{\partial t} \right) + \theta \left( \frac{\partial \rho}{\partial C} \right) \left( \frac{\partial C}{\partial t} \right) - \rho_s q_s^{\setminus} \end{aligned} \quad (1)$$

The Integrated MT3DMS Transport (IMT) process solves the solute transport equation (Zheng and Wang 1999), Eq. 2:

$$\begin{aligned} \left( 1 + \frac{\rho_b K_d^k}{\theta} \right) \left( \frac{\partial (\theta C^k)}{\partial t} \right) \\ = \nabla \left[ \theta \left( D_m^k + \alpha \frac{q}{\theta} \right) \cdot \nabla C^k \right] - \nabla \cdot (q C^k) - q_s^{\setminus} * C_s^k \end{aligned} \quad (2)$$

The governing equation of the heat transport equation (Langevin et al. 2008) is expressed as follows, Eq. 3:

$$\begin{aligned} \left( 1 + \frac{1 - \theta}{\theta} * \frac{\rho C_{psolid}}{\rho_s C_{pfluid}} \right) \left( \frac{\partial (\theta T)}{\partial t} \right) \\ = \nabla \left[ \theta \left( \frac{K_{Tbulk}}{\theta \rho C_{pfluid}} + \alpha \frac{q}{\theta} \right) \cdot \nabla T \right] - \nabla \cdot (q T) - q_s^{\setminus} * T_s \end{aligned} \quad (3)$$

Dynamic viscosity in SEAWAT is developed as a function of only temperature and solute concentration; the general equation is the following term (Langevin et al. 2008) expressed as follows, Eq. 4:

$$\mu = \mu_o + \sum_{k=1}^{NS} \frac{\partial \mu}{\partial C^k} (C^k - C_o^k) + \frac{\partial \mu}{\partial T} (T - T_o) \quad (4)$$

where  $\rho_o$ : fluid density [ $ML^{-3}$ ] at the reference concentration and temperature;  $\mu$ : dynamic viscosity [ $ML^{-1} T^{-1}$ ];  $K_o$ : hydraulic conductivity [ $LT^{-1}$ ];  $h_o$ : hydraulic head [L],  $\rho_b$ : bulk density [ $ML^{-3}$ ],  $\rho_s$ : density of the solid [ $ML^{-3}$ ],  $S_{s,0}$ : specific storage [ $L^{-1}$ ],  $t$ : time [T];  $\theta$ : porosity [-];  $C$ : salt concentration [ $ML^{-3}$ ],  $q$ : specific discharge [ $LT^{-1}$ ],  $q_s^{\setminus}$ : a source or sink [ $T^{-1}$ ],  $D_m^k$ : the molecular diffusion coefficient [ $L^2 T^{-1}$ ] for species  $k$ ;  $\alpha$ : the dispersivity tensor [L];  $K_d^k$ : distribution coefficient of species  $k$  [ $L^3 M^{-1}$ ],  $C^k$ : the concentration of species  $k$  [ $ML^{-3}$ ],  $C_s^k$ : the source or sink concentration [ $ML^{-3}$ ],  $C_{psolid}$ : specific heat capacity of the solid [ $L^2 T^{-2} \text{ } ^\circ K^{-1}$ ],  $C_{pfluid}$ : specific heat capacity of the fluid [ $L^2 T^{-2} \text{ } ^\circ K^{-1}$ ],  $K_{Tbulk}$ : bulk thermal conductivity of the aquifer material [ $ML^3 T^{-2} \text{ } ^\circ K^{-1}$ ],  $T_s$ : source temperature [ $^\circ K$ ];  $\mu$ : dynamic viscosity [ $ML^{-1} T^{-1}$ ];  $\mu_o$ : reference dynamic viscosity [ $ML^{-1} T^{-1}$ ];  $C_o^k$ : the concentration of species  $k$  [ $ML^{-3}$ ];  $T$ : temperature [ $^\circ K$ ]; and  $T_o$ : reference temperature [ $^\circ K$ ].

### Verification of the SEAWAT model for temperature simulation

The finite-difference model SEAWAT (V.4) was tested using a standard benchmark problem by Henry and Hilleke (1972)

for variable-density groundwater flow and solute transport codes. This benchmark problem was designed to represent the coastal zone of a carbonate platform where groundwater flow is affected by variations in salinity and temperature. This benchmark problem used to test the variable-density codes of HST3D (Kipp 1987; 1997) and SUTRA-MS Hughes and Sanford (2004) for temperature and concentration effects. Figure 2a and b presents the boundary of Henry and Hilleke (1972) problem as presented in Dausman et al. (2010), which consists of a rectangular domain representing a confined aquifer 100 cm in length, 100 cm in height, and 100 cm in width; the domain is divided into two rows with 40 columns and 40 layers, each cell dimension equals to  $(\Delta x \times \Delta z \times \Delta y)$  2.50 cm  $\times$  2.50 cm  $\times$  50 cm.

Henry and Hilleke (1972) developed a semi-analytical solution for a couple of groundwater flow and solute transport in a confined aquifer toward a seawater boundary called Henry's problem. This problem is tested using several numerical models. Segol et al. (1975) indicated that the solution to Henry's problem was not exact due to computational reasons. They recalculated Henry's solution with the additional terms and showed that it slightly differed from the original. The analytical solution to Henry's problem was developed assuming a constant dispersion coefficient under steady-state conditions (Guo and Langevin 2002). The Henry problem is used as benchmark solutions by INTERA (1979) using SWIFT; by Voss and Souza (1987) using SUTRA; by Kolditz (1994) using FEFLOW; by Oldenburg and Pruess (1995) using TOUGH2, and by Guo and Langevin (2002) using SEAWAT.

The Henry–Hilleke problem boundary conditions for seawater and temperature are defined in Fig. 2a, b. The left vertical boundary of the land side is assigned by freshwater recharge ( $Q_{IN}$ ) by  $7.20 \text{ m}^3 \text{ day}^{-1}$ , equivalent to a hydrostatic freshwater head. Also, a constant concentration ( $C_{IN}$ ) equals  $0 \text{ mg L}^{-1}$ , with temperatures ranging from 50 at the left bottom corner to  $38.5^\circ \text{C}$  at the left top corner. The right vertical boundary is set at a hydrostatic seawater constant head boundary of 1 m with a density of  $1025 \text{ kg m}^{-3}$ . Also, a constant concentration of  $35,000 \text{ mg L}^{-1}$  with a constant temperature of  $5^\circ \text{C}$  was assigned. The upper and lower model boundaries have no flow; in the non-isothermal case, a specified temperature at the bottom varies from 50 to  $5^\circ \text{C}$  and from  $38.5$  to  $5^\circ \text{C}$  at the top in the direction of the sea (Table 1).

Also, a low hydraulic conductivity value at the top and bottom boundaries of  $432 \text{ m d}^{-1}$  minimizes the convective heat flux from the temperature boundaries. In comparison, the other layers have  $864 \text{ md}^{-1}$ .

The current model results were tested and compared for different considerations and simulations. Figure 3 presents the Henry–Hilleke problem results for salt and temperatures, respectively. Also, it can be observed

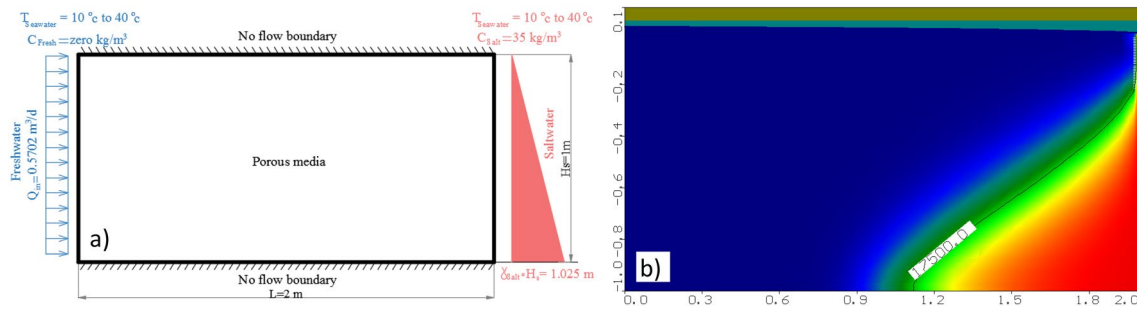


**Fig. 4** Henry's problem for **a** definition sketch and **b** SWI results for Henry's problem using SEAWAT without temperature effect

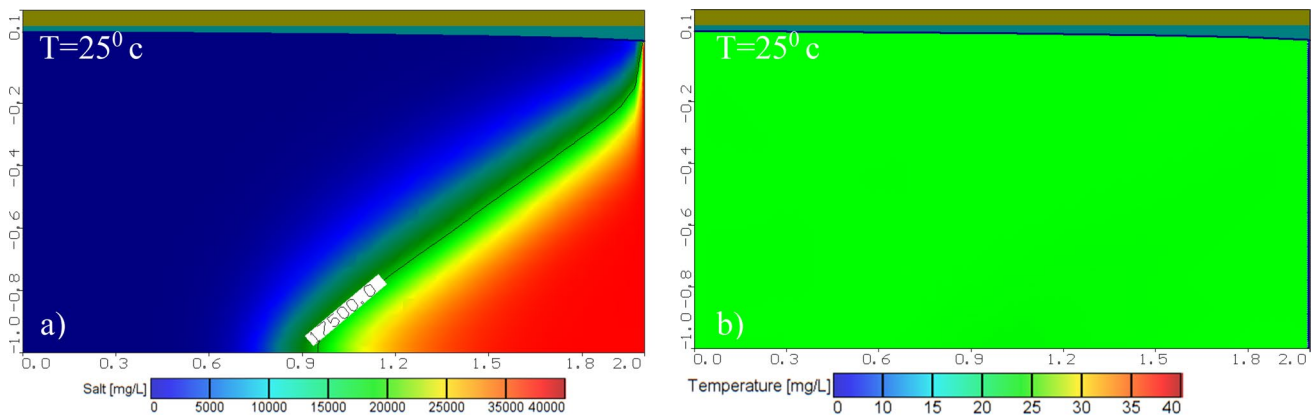


**Fig. 5** Isochlor for Henry's problem at the base case for the distribution of SWI (left) and temperature isochlors 25 °C (right)

that the simulated model results for the Henry–Hilleke problem match well with the results from SUTRA-MS, HST3D (Hughes and Sanford 2004; Thorne and others 2006), and the original Henry and Hilleke (1972) for salt and temperature concentration. The SUTRA-MS results are shown in color with the solid black lines, while Henry and Hilleke numerical solution, has shown as the 50 percent contour and the solid red line, and HST3D results shown as the dashed black line as published by Hughes and Sanford (2004) as presented in Fig. 3.

### Hypothetical modeling of Henry's problem

Henry's problem (1964) is the most popular benchmark test of a variable-density flow application (Klassen and Allen 2017). The accuracy problems in the semi-analytical solution for the original Henry results are not close to those developed by the numerical solutions because the equipotential head contours are not orthogonal to Darcy velocity vectors in Henry's results (Kolditz 1994). These problems confused the other solution to verify the numerical codes due to the uncorrected values of molecular diffusion, which did not correlate with the original Henry value (Voss and Souza 1987). These reasons are derived

from considering two values of molecular diffusion ( $D_m$ ), which is  $2.0571 \text{ m}^2 \text{ d}^{-1}$ . Impermeable strata with no-flow boundaries define the upper and lower boundary. The aquifer is homogenous and isotropic, and the input values used in Henry and Hilleke (1972) problem are summarized in Table 1.

The current model was based on the standard and modified the Henry problem to study saltwater intrusion in two cases: base and heat simulation. The domain of the Henry problem is 2 m horizontal, 1 m vertical, and 10 cm in width; as shown in Fig. 4a, the domain is divided into 41 columns, 20 layers, and two rows with equal cell dimensions of  $25 \text{ cm}^2$  except for the last column at the seaside the length is 0.50 cm. Figure 4a presents the boundary conditions of Henry's problem.

A hydrostatic seawater head fixes the right boundary condition with a constant concentration of 35,000 ppm. In contrast, a constant freshwater flux fixes the left side by  $5.702 \text{ m}^3 \text{ d}^{-1} \text{ m}^{-1}$  while the model head ranges from zero at the seaside. In this case, the model was carried out using a constant dispersion coefficient ( $D_m$ ) based on the assumption that Henry's solution uses a molecular diffusion coefficient of  $0.57024 \text{ m}^3 \text{ day}^{-1} \text{ m}^{-1}$ . The 0.5 isochlor reached  $86.50 \text{ cm}$  from the seaside at the base case (Fig. 4b).

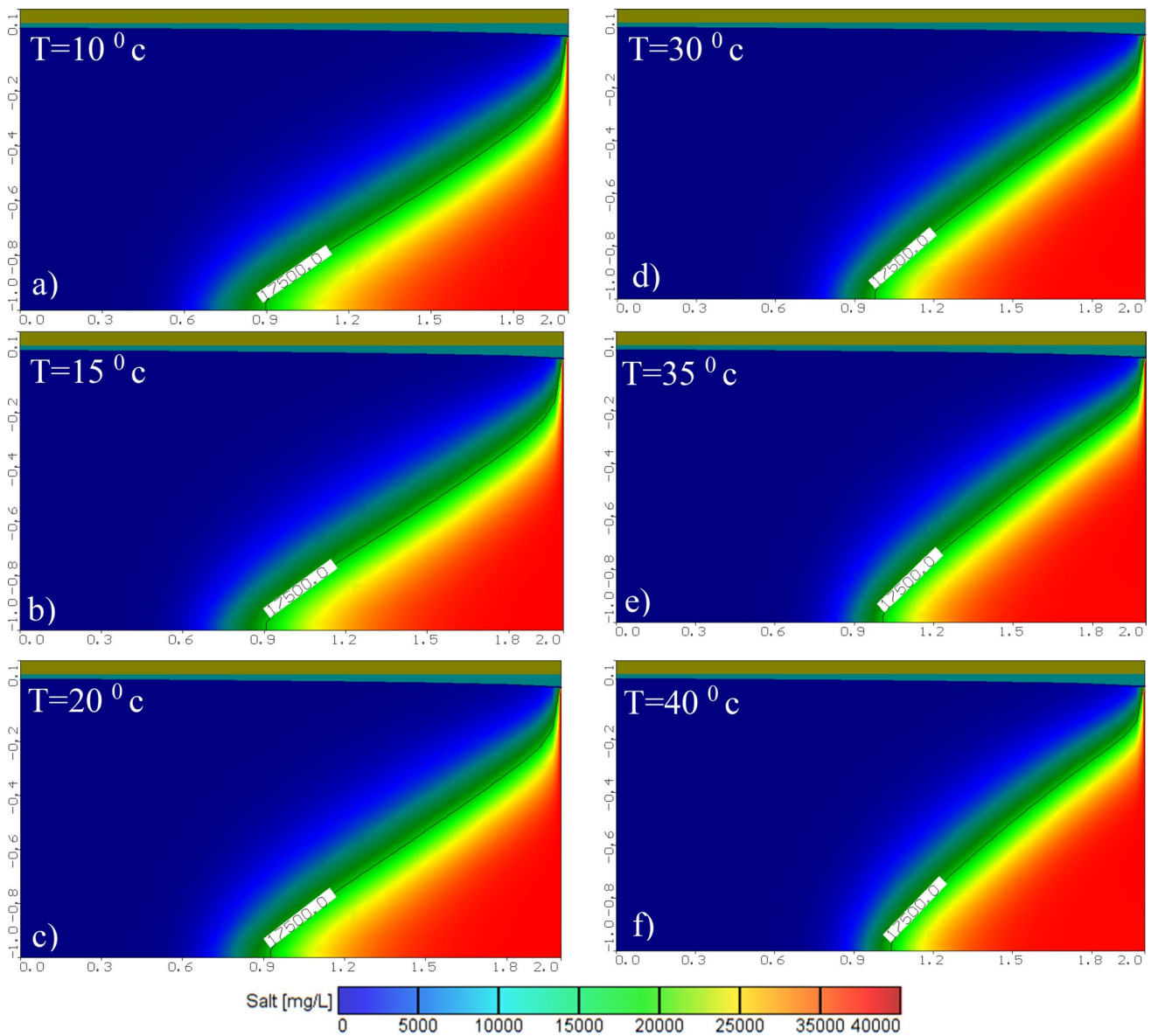


**Fig. 6** Distribution of SWI for Henry's problem by changing the saline water temperature

The current model results were tested and evaluated with the other codes, and a good agreement was given in the results as presented in Fig. 4b.

## Results

### Impact of water temperature on SWI

The model simulated Henry's problem, considering the effect of temperature. The ocean boundary conditions for

temperature and concentration were set along the right side with a constant temperature of 25 degrees Celsius and 35,000 ppm, considering the hydrostatic conditions based on a fluid density at 25 °C. The aquifer's left freshwater influx boundary was also at 25 °C. The thermal effect is included in the SEAWAT model in this case, and the wedge of the saline water intrusion, considering the temperature, is shown in Figs. 5a, b. The intrusion of 0.5 isochlor reached 105 cm from the seawater boundary, compared to 86.5 cm for the case without thermal effect in SEAWAT. This means that the thermal effect led to increased intrusion length.

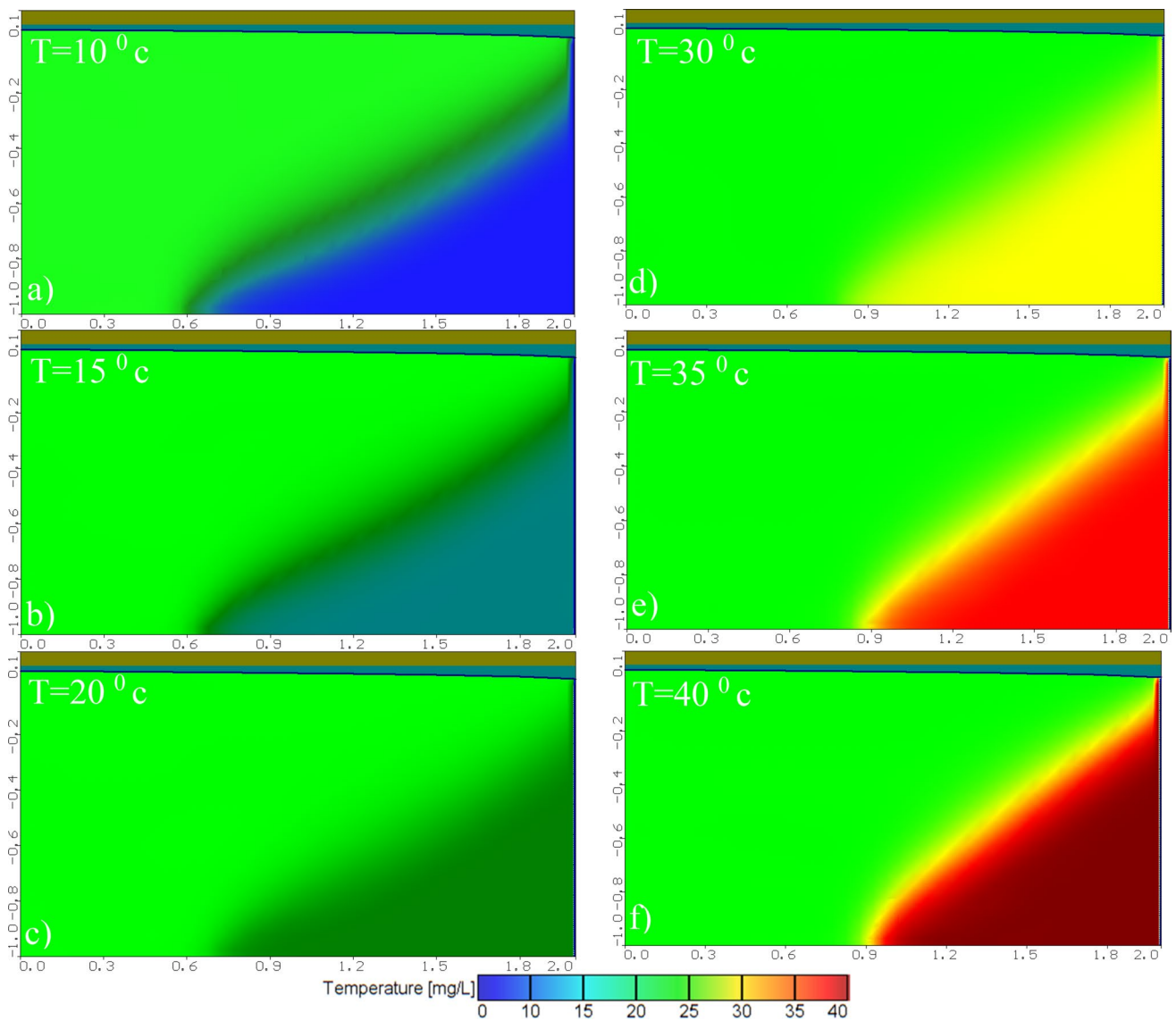


**Fig. 7** Heat Distribution for Henry's problem by changing the saline water temperature

**Impact of increasing the seawater boundary temperature (Scenario 1)**

The numerical model was developed to study the combined effect of concentration and temperature. This scenario was modeled by changing the saline water temperature as a result of climate change by 10 °C, 15 °C, 20 °C, 30 °C, 35 °C, and 40 °C. The model results showed that increasing the saline water temperature increases SWI to 109.50 cm, 108 cm, 107 cm, 105 cm, 98.50, and 95.50 cm compared with 86.50 cm at the base for the effect of concentration only (without temperature effect). The lower the seawater temperature, the

greater is the SWI wedge into the aquifer (see Fig. 6). At the same time, increasing the saline water temperature has more effects on the reduction of the SWI.

The heat distribution in the aquifer increased for the saline water temperature by 10 °C, 15 °C, 20 °C, 30 °C, 35 °C, and 40 °C, respectively, compared to the case without considering the temperature effect in the SEAWAT model, as shown in Fig. 7 and the SWI length.

The relation between the seawater temperatures and SWI length is presented in Fig. 8. The figure shows a decrease in SWI by 26.60%, 24.90%, 23.70%, 18.50%, 13.90%, and 10.40%, for ocean temperature of 10 °C, 15 °C, 20 °C, 30

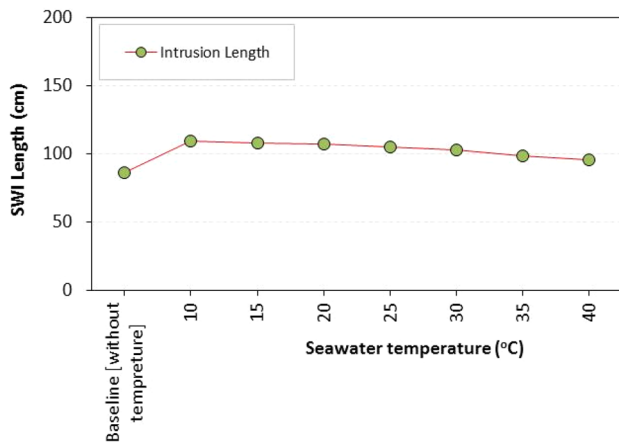


**Fig. 8** Relation between the SWI and temperature of the saline water heads for Henry's problem

°C, 35 °C, and 40 °C, respectively, compared with the base case without including the temperature effect in the SEAWAT model. Increasing the seawater temperature decreases the viscosity of saline water and its hydrostatic force. These leads to a decrease in the SWI wedge in coastal aquifers. The model temperature at 10 °C produced the maximum saline water intrusion length after which the wedge started to decrease again.

Also, the saltwater intrusion repulsion was calculated by  $(L-L_0)/L_0$  to check the aquifer salt situation which the positive sign indicated that the aquifer salt is more than the base case, and this is a negative impact to salt remove while the negative sign represents a positive effect on SWI, where  $L_0$  is the initial SWI length, and  $L$  is the SWI length at the given case.

### Effect of aquifer recharge influx temperature on saltwater intrusion (Scenario 2)

This scenario was modeled by changing the freshwater recharge temperature by 10 °C, 15 °C, 20 °C, 25 °C, 30 °C, 35 °C, and 40 °C, respectively, compared to the base case without considering the temperature effect. Figure 9 shows that the seawater intrusion length reached 88 cm, 92.50 cm, 99 cm, 105 cm, 110.50 cm, 115.50 cm, and 121.50 cm, for temperature 10 °C, 15 °C, 20 °C, 25 °C, 30 °C, 35 °C, and 40 °C, respectively, compared to the base case where the intrusion length was 86.50 cm. This increase in the intrusion length is attributed to the decrease in freshwater density and viscosity by increasing the freshwater temperature, which promotes the seawater intrusion further into the aquifer.

The groundwater heat increased as presented in Fig. 10 for changing the temperature of the boundary condition of the freshwater. The results presented in Fig. 10, which shows the heat distribution, have hydrological importance because heat distribution within the aquifer guides hydrogeologists

for optimum for freshwater abstractions. Whenever the weather is cold, it me be more appropriate to abstract water with relatively warm temperature. The opposite is true in hot weather, where the abstraction of colder water may be better option. This can also lead to energy saving.

Figure 11 presents the relation between the freshwater recharge temperature and SWI length. Increasing the freshwater temperature to 10 °C, 15 °C, 20 °C, 30 °C, 35 °C, and 40 °C, led to increase in SWI by 0.60%, 6.90%, 14.50%, 27.80%, 33.50%, and 40.50%, respectively, compared to the base case where the temperature effect was not considered. The results showed that increasing the aquifer temperature using hot irrigation water in the summer seasons or water injection will decrease the water viscosity and increase SWI in coastal aquifers.

### Effect of the combination between scenarios 1 and 2

This scenario was developed by a combination of rising seawater boundary temperature by 10 °C, 15 °C, 20 °C, 30 °C, 35 °C, and 40 °C and also changing the temperature of freshwater recharge temperature by 10 °C, 15 °C, 20 °C, 30 °C, 35 °C, and 40 °C, respectively. The results showed that the intrusion reached 93.50 cm, 97.50 cm, 100.50 cm, 105 cm, 108 cm, 111 cm, and 114 cm, respectively, as shown in Fig. 12, compared to the base case where the intrusion length was 86.50 cm. Figure 13 is presented an increasing in the heat distribution in the aquifer for the combined of saline water and aquifer freshwater temperature by 10 °C, 15 °C, 20 °C, 30 °C, 35 °C, and 40 °C, respectively, compared to the case without considering the temperature effect. This represents increase in SWI by 8.10%, 12.70%, 16.20%, 24.90%, 28.30%, and 31.80%, respectively as shown in Fig. 14.

The aquifer temperature was increased (Fig. 13) for the combined sea and aquifer temperature by 10 °C, 15 °C, 20 °C, 25 °C, 30 °C, 35 °C, and 40 °C, respectively (Table 2). The relation between the combined seawater with freshwater recharge temperatures and SWI length is presented in (Fig. 14) by 10 °C, 15 °C, 20 °C, 25 °C, 30 °C, 35 °C, and 40 °C, respectively (Table 2).

### Discussion

In implementing engineering prevention measures, it is paramount to increase human awareness regarding the profound impact of climate change on elevating freshwater body temperatures within coastal aquifers. This heightened awareness is indispensable for ensuring the efficacy of these measures and promoting the sustainable utilization of groundwater resources in future planning endeavors (Byrne 1999; Ehtai et al. 2018).

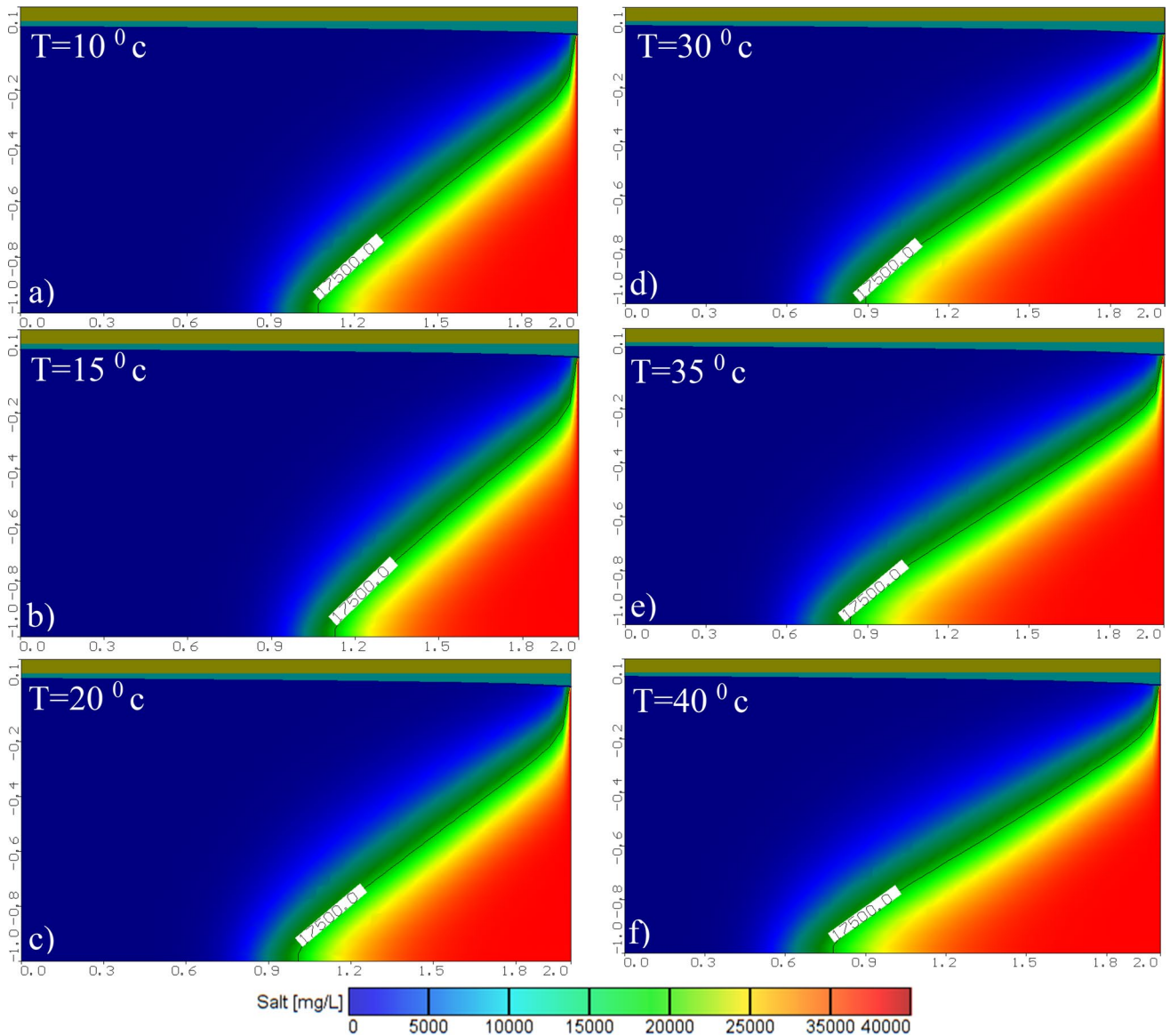


**Fig. 9** Distribution of SWI for Henry's problem by changing the aquifer water temperature

This study unveils the outcomes of Henry's problem in its base case, wherein the 0.5 isochlor of the seawater wedge extends to 86.50 cm from the seaside when the heat effect is not considered in the SEWAT model. Exploring the impact of temperature on SWI, both the freshwater and seawater boundary conditions were both maintained at 25 °C. This increase in boundary temperature resulted in the SWI intrusion extending to 105 cm, which represents a 21.40% increase compared with the baseline case intrusion length of 86.50 cm.

The study further investigated variations in saline water temperatures, ranging from 10 °C to 40 °C, compared to

the base case that has no temperature effect. The SWI length experienced reductions of + 26.60%, + 24.90%, + 23.70%, + 18.50%, + 13.90%, and + 10.40% for seawater boundary temperature of 10 °C, 15 °C, 20 °C, 25 °C, 30 °C, 35 °C, and 40 °C, respectively, compared to the basecase.

Additionally, variations in freshwater recharge boundary temperature, ranging from 10 °C to 40 °C, are explored against the baseline case without temperature influence. The saltwater intrusion repulsion registered increments of + 1.70%, + 6.90%, + 14.50%, + 27.80%, + 33.50%, and + 40.50% corresponding to the temperatures of 10 °C, 15 °C, 20 °C,

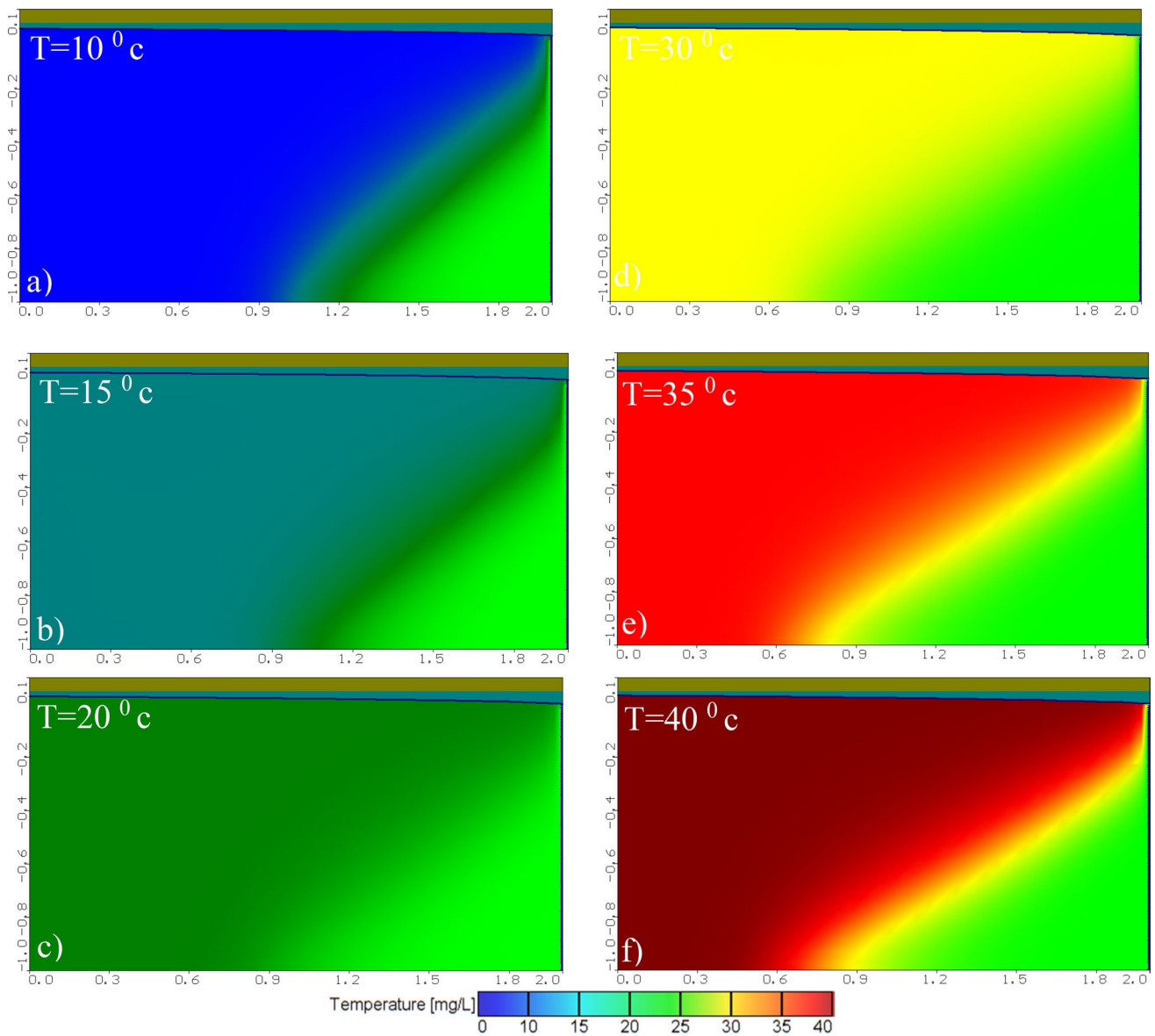


**Fig. 10** Distribution of heat for Henry's problem by changing the aquifer water temperature

25 °C, 30 °C, 35 °C, and 40 °C, respectively, compared to the basecase. The combined impact of seawater temperature and freshwater temperature is also considered, with temperature range of 10°C to 40°C. The temperature-induced changes in the SWI wedge length increase of +8.10%, +12.70%, +16.20%, +24.90%, +28.30%, and +31.80% for temperatures of 10 °C, 15 °C, 20 °C, 25 °C, 30 °C, 35 °C, and 40 °C, respectively, compared to the basecase.

This intricate examination sheds light on the interplay between various temperatures and their cumulative effects on SWI in coastal aquifers. It provides valuable insights

for understanding and managing the complex dynamics of groundwater systems in the face of changing temperature conditions (Fig. 15).

The SWI concentration results without the impact of temperature are in agreement with Al-Charideh (2012) and Abd-Elaty et al. (2021b), while the influence of SWI concentration with temperature results fit with Langevin et al. (2007). Many studies, including Nguyen et al. (2020), applied laboratory experiments and numerical simulations to study the effect of temperature on tidally influenced coastal unconfined aquifers. The study has illuminated the intricate

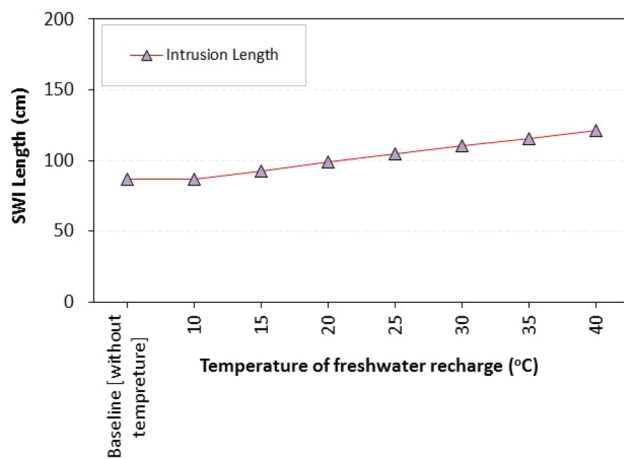


**Fig. 11** Relation between the SWI and temperature of freshwater recharge for Henry's problem

relationship between seawater temperature and key hydrodynamic factors within coastal aquifers. Elevated seawater temperature amplifies hydraulic conductivity, fostering heightened aquifer–ocean mass exchange, intensifying tidally induced seawater circulation, and augmenting submarine groundwater discharge. This phenomenon is particularly pronounced in cold temperate zones, where the significant temperature contrast between seawater and groundwater contributes to enhanced coastal dynamics.

The thermal effect on coastal dynamics is comparably diminished in regions closer to the equator, where the temperature differential is less substantial. In a compelling contrast to the isothermal scenario, our findings reveal a noteworthy upsurge of up to 40% in the tide-induced seawater circulation rate within the intertidal zone when seawater surpasses groundwater in temperature. This underscores the pivotal role of thermal conditions in influencing the intricate dynamics of coastal aquifers, with implications that extend from hydraulic conductivity to tidal circulation rates, providing valuable insights for comprehending and managing these complex systems. Pu et al. (2021) showed that the seawater temperature increases or freshwater temperature decreases, the freshwater–seawater interface retreats seaward, and thus, the freshwater storage increases. This occurs because of temperature-induced changes to the fluid density and aquifer hydraulic conductivity. In other words, warmer seawater caused the seawater to retreat seaward, whereas the warmer freshwater induced further seawater intrusion compared to the isothermal case.

Cogswell and Heiss (2021) studied the impact of controlling the climate and seasonal temperature on the

biogeochemical transformations in unconfined coastal aquifers; the results indicated that the efficiency of nitrate removal increased from 5 to 88% by increasing the freshwater temperature from 5 to 35 °C. Blanco-Coronas et al. (2022) showed that the temperature distribution in coastal aquifers is highly sensitive to natural changes or those induced by humans. The position of the freshwater–saltwater interface and the thermal plume depends on groundwater recharge, which, in turn, depends on climate variability and/or water management. Abd-Elaty et al. (2023) developed a new approach using the Abstraction of saline water, Desalination, Cooling the desalinated water, and Injection into the aquifer (ADCI) strategy. The results showed that coastal regions' freshwater recharge is sensitive to the thermal regime. Xin et al. (2023) studied the impact of decreasing groundwater temperature relieving seawater intrusion in coastal aquifers. The results showed about 47.4% with groundwater cooling and without fresh groundwater exploitation. Furthermore, without incurring further seawater intrusion, groundwater cooling can lead to 35.7% of fresh submarine groundwater discharge (FSGD) exploitation.

This study and existing literature underscore the pivotal role of temperature in significantly influencing saltwater intrusion (SWI) dynamics within coastal aquifers. The findings presented here bear critical implications for decision-makers involved in future planning, management, and design processes to safeguard freshwater storage against climate change and rising sea and ocean temperatures, recognized as key drivers impacting SWI.

Furthermore, our study reveals a noteworthy observation: coastal aquifers in elevated regions with higher seawater temperatures exhibit a more pronounced positive correlation than those with lower temperatures. This phenomenon can be attributed to the inverse relationship between seawater temperature and saline water density, coupled with a reduction in the hydrostatic force of seawater as temperatures increase. These insights contribute to a deeper understanding of the complex interactions in coastal aquifers, providing valuable guidance for decision-makers grappling with changing environmental conditions. However, this option can increase the groundwater recharge to the sea and decrease the fresh groundwater storage in coastal areas, which the saline water interface will balance as a base case as presented by Pu et al. (2021).

Moreover, the practical application for the irrigation process in the morning or at night with low water temperatures could control the coastal aquifer salinity and support the freshwater resources in coastal aquifers. Cooling the freshwater is an energy requirement and could preferably be done

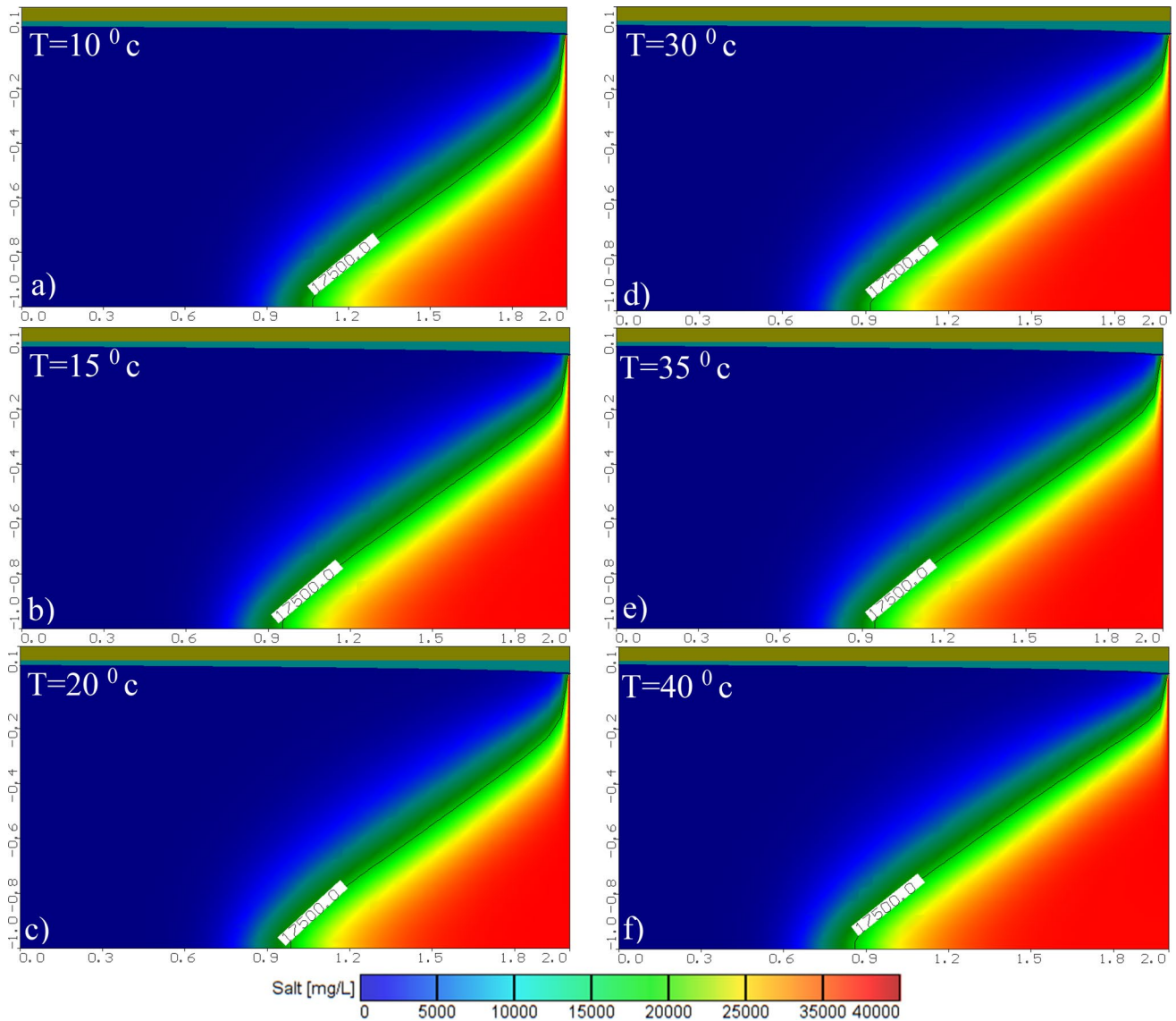


**Fig. 12** Distribution of SWI for Henry's problem by a combination of the seawater and aquifer water temperature

during cold seasons in winter. Also, a positive heat transfer (from hot to cold objects) would allow groundwater to be cooled through natural and/or engineering heat exchange (a widely-used thermal utilization technology) (Pu et al. 2021).

This study acknowledges limitations inherent in its approach, particularly in extrapolating the temperature effect to a real case study to demonstrate its impact on saltwater intrusion (SWI) in coastal aquifers. While the insights gained are valuable, it is imperative to recognize that the practical application of temperature influence necessitates thoroughly examining feasibility and economic considerations.

Expanding the scope to large hydrogeological systems by implementing a three-dimensional (3D) model introduces another layer of complexity. Assessing aquifers–ocean salinity hazards on this scale requires meticulous attention to detail and understanding the intricate dynamics at play.

Furthermore, the transition to practical applications in coastal regions poses a challenge, particularly in hot climates where cooling freshwater may rely on alternative energy sources. Addressing this challenge is crucial for the

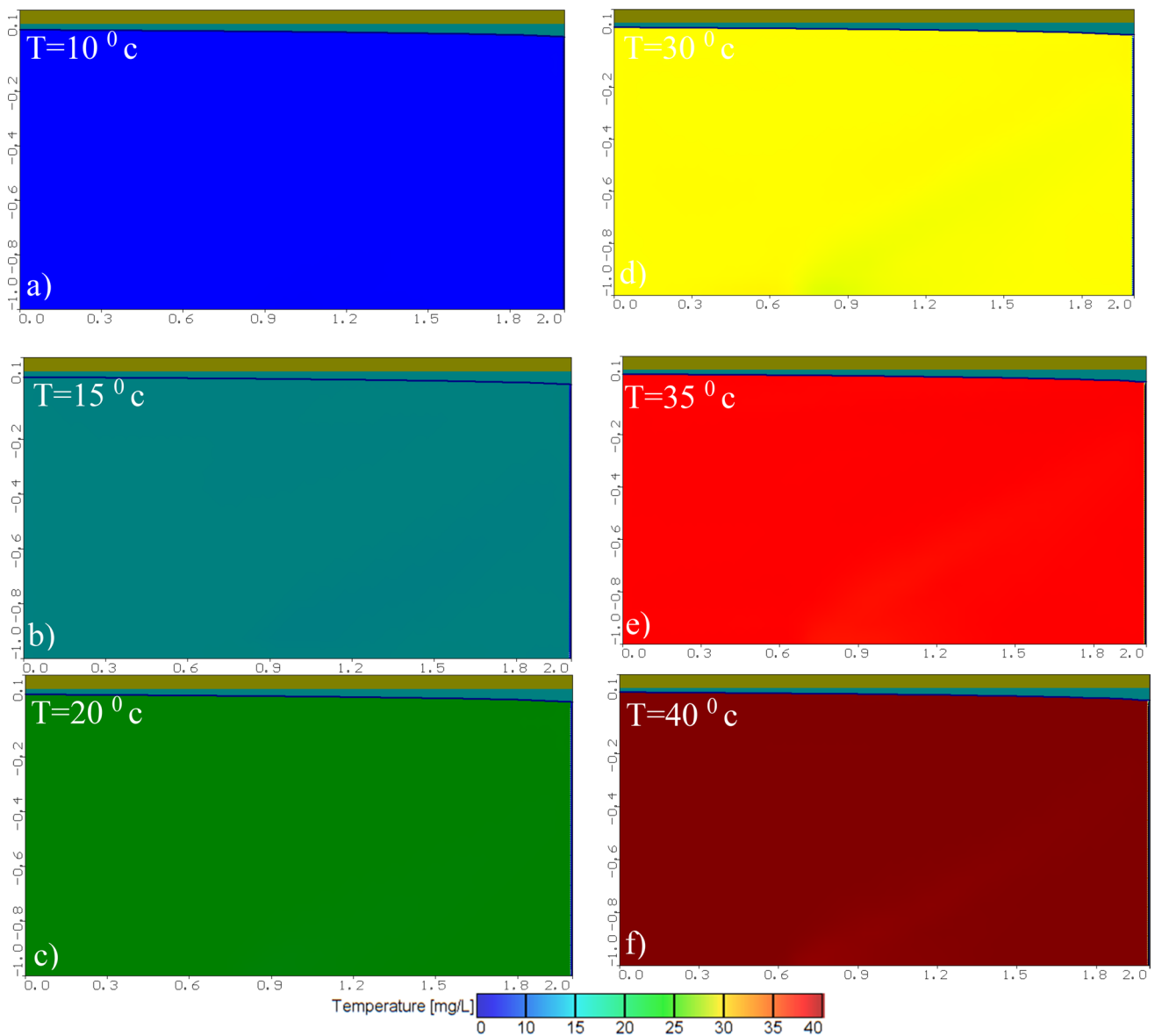


**Fig. 13** The temperature distribution for Henry's problem by combining the seawater and aquifer freshwater temperatures

broader implementation of this technique, and exploring viable energy alternatives becomes integral to its feasibility in real-world scenarios. While the study provides valuable insights, its practical application demands a comprehensive consideration of economic, logistical, and energy-related factors.

### Conclusion

Groundwater contamination by saltwater intrusion (SWI) is a formidable challenge in coastal regions globally. This study delves into the dynamic shifts in aquifer boundary conditions triggered by seawater and freshwater boundary temperature

fluctuations attributed to climate change and heightened ground and irrigation water temperatures. Employing the variable-density SEAWAT code, we simulated the temperature effect in a hypothetical model of the Henry problem, exploring three scenarios: seawater temperature variations, freshwater aquifer recharge temperature variations, and a combination of both.

Our results illuminate the substantial impact of combining seawater temperature and freshwater recharge boundary temperature variations, ranging from 10 to 40 °C, compared to the baseline without temperature effect. Salinity concentrations surged by +8.10%, +12.70%, +16.20%, +21.40%, +24.90%, +28.30%, and +31.80% for temperatures of 10 °C, 15 °C, 20 °C, 25 °C, 30 °C, 35 °C, and 40

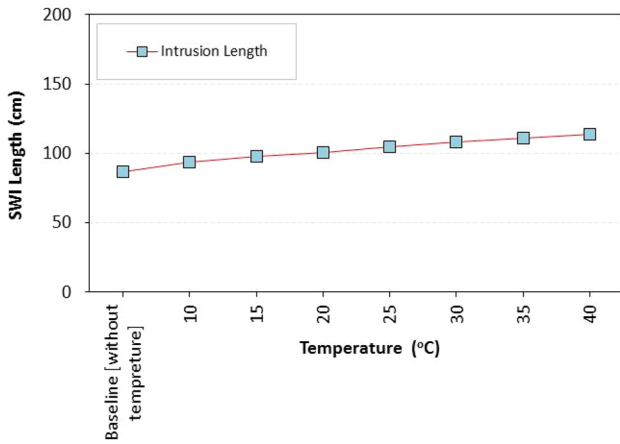


**Fig. 14** Relation between the SWI and temperature of saline water with freshwater recharge for Henry's problem

°C, respectively, compared to basecase. These findings underscore the urgency of addressing climate-induced and artificially induced forces, as they significantly influence coastal aquifer salinity, necessitating robust control measures.

The imperative for future groundwater modeling is emphasized, urging consideration of landside and ocean boundaries temperatures in developmental planning,

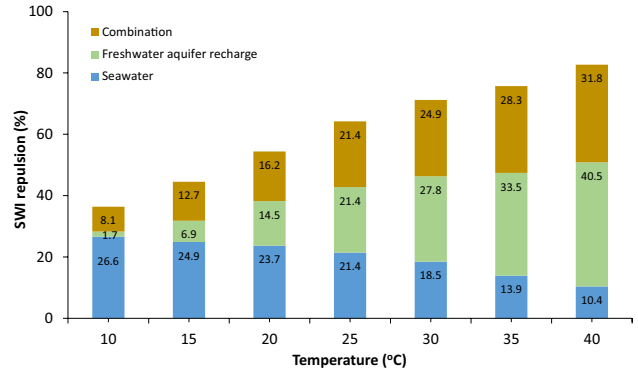


**Fig. 15** Saltwater intrusion repulsion under different scenarios of seawater and groundwater recharge temperature for three cases

aquifer operations, and water resource management. This holistic approach is crucial to safeguarding freshwater from pollution and upholding public health standards in changing environmental conditions.

However, it is crucial to exercise caution in applying the findings, particularly in 3D simulations, and to meticulously assess the feasibility and economic dimensions of temperature influence on freshwater for practical applications. Furthermore, the study calls for additional research on the impact of aquifers–ocean salinity hazards, especially

**Table 2** Results of numerical analysis for Henry's problem

Case	Temperature (°C)		SWI length (cm)	SWI repulsion (%)
	Seawater	Freshwater		
Base (concentration)	–	–	86.5	–
Base (temperature)	25	25	105	21.40
Saline water (scenario 1)	10	25	109.5	26.60
	15		108	24.90
	20		107	23.70
	30		102.5	18.50
	35		98.5	13.90
	40		95.5	10.40
	Freshwater recharge (scenarios 2)	25	10	87
		15	92.5	6.90
		20	99	14.50
		30	110.5	27.80
		35	115.5	33.50
		40	121.5	40.50
Combination between scenarios 1 and 2	10	10	93.5	8.10
	15	15	97.5	12.70
	20	20	100.5	16.20
	30	30	108	24.90
	35	35	111	28.30
	40	40	114	31.80

in regions facing high-stress water supply challenges. Collectively, these efforts contribute to a more comprehensive understanding and effective management of the intricate dynamics associated with coastal aquifers.

**Acknowledgements** The authors thank the Department of Water and Water Structures Engineering, Faculty of Engineering, Zagazig University. Alban Kuriqi acknowledges the Foundation for Science and Technology's support through funding UIDB/04625/2020 from the research unit CERIS.

**Authors contributions** IAE and AK helped in conceptualization, methodology, investigation, formal analysis, and data curation. IAE, AK, and AA helped in visualization, writing—original draft, writing—review & editing, resources, and supervision.

**Funding** This study did not receive any funding.

**Availability of data and materials** Upon request.

**Code availability** Upon request.

## Declarations

**Conflicts of interest** The authors declare no conflict of interest.

**Ethics approval** Not applicable.

**Consent to participate** Yes.

**Consent for publication** Yes.

**Open Access** This article is licenced under a Creative Commons Attribution 4.0 International License, which permits use, sharing, adaptation, distribution, and reproduction in any medium or format, as long as you give appropriate credit to the original author(s) and the source, provide a link to the Creative Commons licence, and indicate if changes were made. The images or other third-party material in this article are included in the article's Creative Commons licence, unless indicated otherwise in a credit line to the material. If material is not included in the article's Creative Commons licence and your intended use is not permitted by statutory regulation or exceeds the permitted use, you will need to obtain permission directly from the copyright holder. To view a copy of this licence, visit <http://creativecommons.org/licenses/by/4.0/>.

## References

- Abd-Elaty I, Shahawy AEL, Santoro S, Curcio E, Straface S (2021a) Effects of groundwater abstraction and desalination brine deep injection on a coastal aquifer. *Sci Total Environ* 795:148928. <https://doi.org/10.1016/j.scitotenv.2021.148928>
- Abd-Elaty I, Straface S, Kuriqi A (2021b) Sustainable saltwater intrusion management in coastal aquifers under climatic changes for humid and hyper-arid regions. *Ecol Eng* 171:106382. <https://doi.org/10.1016/j.ecoleng.2021.106382>
- Abd-Elaty I, Kushwaha NL, Grismer ME, Elbeltagi A, Kuriqi A (2022) Cost-effective management measures for coastal aquifers affected by saltwater intrusion and climate change. *Sci Total Environ* 836:155656. <https://doi.org/10.1016/j.scitotenv.2022.155656>
- Abd-Elaty I, Kuriqi A, Garrote L (2023) Freshwater cooling injection to mitigate saltwater intrusion and support sustainable groundwater management. *Desalination* 564:116776. <https://doi.org/10.1016/j.desal.2023.116776>
- Abd-Elaty I, Kuriqi A, Ramadan EM, Ahmed AA (2024) Hazards of sea level rise and dams built on the River Nile on water budget and salinity of the Nile Delta aquifer. *J Hydrol Region Stud* 51:101600. <https://doi.org/10.1016/j.ejrh.2023.101600>
- Agren J, Svensson R (2007) Postglacial land uplift model and system definition for the new Swedish height system RG 2000. Gävle, Lantmäteriet
- Al-Charideh A (2012) Recharge rate estimation in the Mountain karst aquifer system of Figeih spring, Syria. *Environ Earth Sci* 65:1169–1178. <https://doi.org/10.1007/s12665-011-1365-5>
- Bear J, Cheng AH-D (2010) Modeling groundwater flow and contaminant transport. Springer, Berlin
- Bear J (2012) *Hydraulics of groundwater*. Courier Corporation
- Benz SA, Bayer P, Blum P (2017) Global patterns of shallow groundwater temperatures. *Environ Res Lett* 12:034005. <https://doi.org/10.1088/1748-9326/aa5fb0>
- Blanco-Coronas AM, Calvache ML, López-Chicano M, Martín-Montañés C, Jiménez-Sánchez J, Duque C (2022) Salinity and temperature variations near the freshwater-saltwater interface in coastal aquifers induced by ocean tides and changes in recharge. *Water* 14:2807
- Byrne MJ (1999) Groundwater nutrient loading in Biscayne Bay, Biscayne National Park. Florida International University, Florida
- Cogswell C, Heiss JW (2021) Climate and seasonal temperature controls on biogeochemical transformations in unconfined coastal aquifers. *J Geophys Res Biogeosci* 126(12):1–21. <https://doi.org/10.1029/2021JG006605>
- Carrasco AR, Ferreira Ó, Roelvink D (2016) Coastal lagoons and rising sea level: a review. *Earth Sci Rev* 154:356–368. <https://doi.org/10.1016/j.earscirev.2015.11.007>
- Dausman AM, Langevin CD, Thorne Jr, DT, Sukop MC (2010) Application of SEAWAT to select variable- density and viscosity problems: U.S. geological survey, scientific investigations report 2009–5028, 31 p.
- Ehtiat M, Jamshid Mousavi S, Srinivasan R (2018) Groundwater modeling under variable operating conditions using SWAT, MODFLOW and MT3DMS: a catchment scale approach to water resources management. *Water Resour Manage* 32:1631–1649. <https://doi.org/10.1007/s11269-017-1895-z>
- Guo W, Langevin CD (2002) User's guide to SEAWAT; a computer program for simulation of three-dimensional variable-density ground-water flow.
- Henry HR (1964) Effect of dispersion on salt encroachment in coastal aquifers. U.S. Geological Survey Water-Supply, Paper 1613-C70-84
- Henry HR, Hilleke JB (1972) Exploration of multiphase fluid flow in a saline aquifer system affected by geothermal heating. Alabama Univ, University (USA)
- IPCC (2014) Climate change 2014: synthesis report. Contribution of Working Groups I, II and III to the Fifth Assessment Report of the Intergovernmental Panel on Climate Change Core Writing Team, R.K. Pachauri and L.A. Meyer (eds.) IPCC, Geneva, Switzerland, pp 151
- Hughes JD, Sanford WE (2004) SUTRA–MS: a version of SUTRA Modified to Simulate Heat and Multiple-solute Transport. US Geological Survey, Reston, VA
- INTERA E (1979) Revision of the documentation for a model for calculating effects of liquid waste disposal in deep saline aquifers. US Geol Surv Water Res Publ:79–96.
- Kipp KL Jr (1987) HST3D—A computer code for simulation of heat and solute transport in three-dimensional ground-water flow systems: U.S. Geological Survey Water-Resources Investigations Report 86-4095, 517 p.
- Kipp KL Jr (1997) HST3D—Guide to the revised heat and solute transport simulator: HST3D—Version 2: U.S. Geological Survey Water-Resources Investigations Report 97-4157, p 149

- Klassen J, Allen DM (2017) Assessing the risk of saltwater intrusion in coastal aquifers. *J Hydrol* 551:730–745. <https://doi.org/10.1016/j.jhydrol.2017.02.044>
- Kolditz O (1994) Benchmarks for numerical groundwater simulations. Diersch HJ, FEFLOW User's Manual, Release 4:5.1–5.129.
- Langevin CD, Shoemaker WB, Guo W (2003) MODFLOW-2000, the U.S. Geological Survey modular ground-water model—Documentation of the SEAWAT-2000 version with the variable-density flow process (VDF) and the integrated MT3DMS transport process (IMT): U.S. Geological Survey Open-File Report 03-426, p 43
- Langevin CD, Thorne Jr DT, Dausman AM, Sukop MC, Guo W (2007) SEAWAT Version 4: a computer program for simulation of multi-species solute and heat transport
- Langevin CD, Thorne Jr DT, Dausman AM, Sukop MC, Guo W (2008) SEAWAT version 4: a computer program for simulation of multi-species solute and heat transport. Geological Survey (US)
- Langevin CD (2007) SEAWAT: a computer program for simulation of variable-density groundwater flow and multi-species solute and heat transport.
- Mazhar S, Pellegrini E, Contin M, Bravo C, De Nobili M (2022) Impacts of salinization caused by sea level rise on the biological processes of coastal soils - A review. *Front Environ Sci* 10:909415. <https://doi.org/10.3389/fenvs.2022.909415>
- Nandimandalam JR, Sharma K, Alagappan R (2023) Preliminary investigation of saline water intrusion (SWI) and submarine groundwater discharge (SGD) along the south-eastern coast of Andhra Pradesh, India, using groundwater dynamics, sea surface temperature and field water quality anomalies. *Environ Sci Pollut Res* 30:26338–26356. <https://doi.org/10.1007/s11356-022-23973-y>
- Nguyen TTM, Yu X, Pu L, Xin P, Zhang C, Barry DA, Li L (2020) Effects of temperature on tidally influenced coastal unconfined aquifers. *Water Resour Res*. <https://doi.org/10.1029/2019WR026660>
- Oldenburg CM, Pruess K (1995) Dispersive transport dynamics in a strongly coupled groundwater-brine flow system. *Water Resour Res* 31:289–302
- Pu L, Xin P, Yu X, Li L, Barry DA (2021) Temperature of artificial freshwater recharge significantly affects salinity distributions in coastal confined aquifers. *Adv Water Resour* 156:104020. <https://doi.org/10.1016/j.advwatres.2021.104020>
- Rosegrant MW, Cai X, Cline SA (2002) World water and food to 2025: dealing with scarcity. *Intl Food Policy Res Inst*
- Sanford WE, Konikow LF (1985) A two-constituent solute-transport-model for ground-water having variable density. U.S. Geological Survey Water-Resources Investigations Report 85-4279, p 88
- Segol G, Pinder GF, Gray WG (1975) A Galerkin-finite element technique for calculating the transient position of the saltwater front. *Water Resour Res* 11:343–347
- Simpson MJ, Clement TP (2004) Improving the worthiness of the Henry problem as a benchmark for density-dependent groundwater flow models. *Water Resour Res* 40.
- Thorne D, Langevin CD, Sukop MC (2006) Addition of simultaneous heat and solute transport and variable fluid viscosity to SEAWAT. *Comput Geosci* 32:1758–1768. <https://doi.org/10.1016/j.cageo.2006.04.005>
- Todd DK, Mays LW (2004) *Groundwater hydrology*. Wiley
- Van Lopik JH, Hartog N, Zaadnoordijk WJ, Cirkel DG, Raouf A (2015) Salinization in a stratified aquifer induced by heat transfer from well casings. *Adv Water Resour* 86:32–45. <https://doi.org/10.1016/j.advwatres.2015.09.025>
- Voss CI (1984) A finite-element simulation model for saturated-unsaturated, fluid-density-dependent ground-water flow with energy transport or chemically-reactive single-species solute transport: U.S. Geological Survey Water- Resources Investigations Report 84-4369, p 409
- Voss CI, Souza WR (1987) Variable density flow and solute transport simulation of regional aquifers containing a narrow freshwater-saltwater transition zone. *Water Resour Res* 23:1851–1866
- Xin P, Pu L, Lao C, Yu X, Bo Y, Zhou F, Yuan S, Tang H, Li L (2023) Decreasing groundwater temperature relieves seawater intrusion in coastal aquifers. *Fundam Res*. <https://doi.org/10.1016/j.fmre.2023.07.007>
- Yu X, Xin P, Pu L (2022) Thermal effects on flow and salinity distributions in heterogeneous coastal aquifers with fixed-flux inland boundaries. *Front Environ Sci* 10:1002587. <https://doi.org/10.3389/fenvs.2022.1002587>
- Zheng C, Wang PP (1999) MT3DMS: a modular three-dimensional multispecies transport model for simulation of advection, dispersion, and chemical reactions of contaminants in groundwater systems; documentation and user's guide
- Zhu S, Zhou Z, Werner AD, Chen Y (2023) Experimental analysis of intermittent pumping effects on seawater intrusion. *Water Resour Res* 59:e2022WR032269

**Publisher's Note** Springer Nature remains neutral with regard to jurisdictional claims in published maps and institutional affiliations.